Journal of Clinical Neuroscience xxx (2010) xxx–xxx

Contents lists available at ScienceDirect

Journal of Clinical Neuroscience

journal homepage: www.elsevier.com/locate/jocn

Laboratory Study

Slope analysis of somatosensory evoked potentials in spinal cord injury for detecting contusion injury and focal demyelination

Gracee Agrawal [a], David Sherman [b], Anil Maybhate [a,*], Michael Gorelik [c], Douglas A. Kerr [c], Nitish V. Thakor [a], Angelo H. All [a,c]

[a] Department of Biomedical Engineering, Johns Hopkins University School of Medicine, 720 Rutland Avenue, Traylor 710B, Baltimore, Maryland 21205, USA
[b] Infinite Biomedical Technologies LLC, 3600 Clipper Mill Rd, Suite 410, Baltimore, Maryland 21211, USA
[c] Department of Neurology, Johns Hopkins University School of Medicine, Baltimore, Maryland 21205, USA

ARTICLE INFO

Article history:
Received 7 February 2010
Accepted 17 February 2010
Available online xxxx

Keywords:
Contusion
Experimental autoimmune encephalomyelitis
Rat model
Somatosensory evoked potentials
Spinal cord injury

ABSTRACT

In spinal cord injury (SCI) research there is a need for reliable measures to determine the extent of injury and assess progress due to natural recovery, drug therapy, surgical intervention or rehabilitation. Somatosensory evoked potentials (SEP) can be used to quantitatively examine the functionality of the ascending sensory pathways in the spinal cord. A reduction of more than 50% in peak amplitude or an increase of more than 10% in latency are threshold indicators of injury. However, in the context of injury, SEP peaks are often obscured by noise. We have developed a new technique to investigate the morphology of the SEP waveform, rather than focusing on a small number of peaks. In this study, we compare SEP signals before and after SCI using two rat models: a contusion injury model and a focal experimental autoimmune encephalomyelitis model. Based on mean slope changes over the signal, we were able to effectively differentiate pre-injury and post-injury SEP values with high levels of sensitivity (83.3%) and specificity (79.2%).

1. Introduction

Based on an average annual incidence of approximately 40 cases per million people in the United States, it is estimated that more than 12 000 people survive a spinal cord injury (SCI) each year.[1] Around 258 000 people in the United States are reportedly living with the devastating effects of an SCI.[1] On the basis of etiology, there are two general types of SCI: traumatic (due to blunt mechanical impact) and non-traumatic (due to vascular, ischemic or neoplastic causes, or immunological disorders). Traumatic SCI accounts for nearly 60% of all injuries to the spinal cord.[2]

The number of spared axonal fibers and the degree to which they are demyelinated play important roles in determining the residual functionality present after SCI. "Anatomically incomplete" injuries are those in which a number of spared but demyelinated axons remain intact across the lesion, without electrophysiological responses.[3–6] Even a small number of spared fibers remaining after SCI can greatly improve the quality of life of SCI patients. Development of therapeutic strategies to reduce secondary injury, and to remyelinate spared, demyelinated axons has generated considerable interest in the past.[7–9] When evaluating any therapeutic approach for SCI, a suitable SCI animal model and reliable monitoring measures are essential, to allow calibration of the severity of the SCI and monitoring of the progress of injury and extent of recovery.[10,11]

A popular animal model of SCI for blunt contusion injuries is a rat model with injury induced using the New York University (NYU) impactor,[12] which is known to reliably emulate the pathophysiology seen in humans after SCI.[13] In this model, some neuronal tissue remains intact along the periphery of the primary site of injury,[13] similar to the situation in humans after blunt injury.[3]

A chemically mediated SCI model is a targeted approach to simulate specific aspects of SCI-like demyelination, inflammation, ischemia or immunological disorders.[14] A focal demyelinating lesion can be induced in the spinal cord of the rat experimental autoimmune encephalomyelitis (EAE) model by administering inflammatory factors directly into the spinal cord of the immunized rat.[15] This model is analogous to the human paralyzing disorder transverse myelitis, which often arises idiopathically or in association with multiple sclerosis.

Various outcome measures for animal models can be used to assess changes due to endogenous recovery, drug therapy, surgical intervention or rehabilitation. Behavioral tests can be used to examine functional recovery in laboratory animals after SCI; however, such tests are often subjective. In contrast, electrophysiological techniques present an objective means for quantitative, non-invasive, accurate assessment of the integrity of neural pathways. Somatosensory evoked potential (SEP) is the electrophysiological

* Corresponding author. Tel.: +1 443 287 6341; fax: +1 410 502 9814.
E-mail address: anil@jhmi.edu (A. Maybhate).

0967-5868/$ - see front matter © 2010 Elsevier Ltd. All rights reserved.
doi:10.1016/j.jocn.2010.02.005

response of the nervous system to electrical stimulation of a peripheral nerve. SEPs can be used to examine the functionality of the ascending sensory pathways, and allow longitudinal measurements. In a number of SCI studies, SEP values have been correlated with neurological deficit scores.[16–21] Unfortunately, no detection standards exist for SEPs; however, a general rule for indicating possible tissue damage has been widely adopted: a reduction of more than 50% in peak and inter-peak amplitudes or an increase of more than 10% in latency with respect to baseline are considered indicative of significant likelihood of injury.[22,23] However, peaks in the SEP waveform are often obscured by noise and may even be indistinguishable in some injuries. This necessitates human intervention for the detection of peaks, rendering the process subject to error and inter-observer variability. This problem prompted us to develop a new technique for quantifying the morphology of the SEP waveform as a whole, rather than just focusing on a few salient peaks.[24] The technique is largely borrowed from shape analysis tools in the field of image processing.[25]

In this paper, we introduce the slope analysis technique for SEPs and present the results of our studies in two rodent SCI models (a contusion model and a focal EAE model).

2. Materials and methods

All experimental procedures were approved by the Institutional Animal Care and Use Committee of Johns Hopkins University. Principles of laboratory animal care as outlined in the National Institutes of Health publication no. 85–23 (revised 1985) were followed.

2.1. Animals

Adult female Fischer rats (n = 12; 200–220 g; Charles River Laboratories, Raleigh, NC, USA) were used for the contusion model, and adult female Lewis rats (n = 12; 200–220 g; Charles River Laboratories) were used for the focal EAE model. The rats were housed individually in cages and had free access to food and water.

2.2. Anesthesia

Anesthesia for all surgical procedures, except SEP recording, was established using a mixture of 45 mg/mL ketamine and 5 mg/mL xylazine administered via intraperitoneal injection.

For SEP recording, anesthesia was established by placing the rat in a transparent chamber with 3% isoflurane gas in room air until the onset of drowsiness. The rat's mouth and nose were then covered with an anesthesia mask with a close-fitting rodent-size diaphragm. A mixture of 1.5% isoflurane, 80% oxygen and room air was delivered to the mask at a rate of 2 L/min to maintain anesthesia. The mask was connected to a C-Pram circuit designed to deliver and evacuate the gas through one tube.

That the level of anesthesia was adequate was confirmed by monitoring the corneal reflex and hindlimb withdrawal to painful stimuli. Rats continued spontaneous breathing and the depth of anesthesia was maintained throughout the experiment. Throughout the entire experiment, rats were placed on a homeothermic blanket system (Harvard Apparatus; Edenbridge, Kent, UK) to maintain their body temperature at 37 ± 0.5 °C, measured using a rectal probe. Lacrilube ophthalmic ointment (Allergan Pharmaceuticals; Irvine, CA, USA) was applied to the rats' eyes to prevent drying.

2.3. Injury

2.3.1. Contusion injury

Following anesthesia, each rat's dorsal region was shaved and aseptically prepared with chlorhexidine (Phoenix Pharmaceuticals; St. Joseph, MO, USA). A midline incision was made along the thoracic vertebrae and the skin was opened. The paravertebral muscles in the region of interest (T6–T12) were retracted. A laminectomy was performed at thoracic vertebra T8 to expose the dorsal surface of the spinal cord underneath, without opening the dura mater. The spinous processes of the vertebrae at T6 and T12 were secured in stabilization clamps to reduce movement of the spinal column during the impact. The impact rod was centered above the exposed part of the spinal cord at the T8 level. The rod was slowly lowered until it came into contact with the dura. This event was detected using an alarm triggered by the completion of an electrical circuit. The exposed dorsal surface of the spinal cord at the T8 level was then contused with the NYU device by dropping the 10 g rod with a flat circular cross-section from a predetermined height (6.25, 12.5, 25.0 or 50.0 mm). The control group underwent only laminectomy with no contusion. Various biomechanical parameters, such as the impact velocity of the rod, the distance of cord compression, the cord compression rate, and the dynamic force applied to the cord were precisely monitored using a computer, and there was <0.05% variation in these values.

2.3.2. Focal autoimmune encephalomyelitis lesion

Recombinant myelin oligodendrocyte glycoprotein (rMOG; Biogen-Idec; Cambridge, MA, USA) corresponding to the N-terminal sequence of rat MOG (amino acids 1 to 125) was emulsified in Freund's incomplete adjuvant (IFA) as a 1:1 mixture (Inject IFA; Pierce, Rockford, IL, USA). Then 100 μL (50 μg per rat, diluted in saline) of this emulsified MOG-IFA mixture was injected subcutaneously at two sites near the base of the tail, one on each side (50 μL per injection, to minimize backflow). After 18 days of MOG sensitization, the rats were anesthetized, then their dorsal region was shaved and aseptically prepared with chlorhexidine. A midline incision was made along the thoracic vertebrae and the skin was opened. The paravertebral muscles in the region of interest (T6–T12) were retracted. A laminectomy was performed at thoracic vertebrae T7–T9 to expose the dorsal surface of the spinal cord underneath without opening the dura mater. The T6–T12 segments of the spinal column were stabilized in a stereotaxic frame, then a Hamilton needle (31G) was used to bilaterally inject cytokines (2 × 2 μL; 250 ng of tumor necrosis factor α, 150 U of interferon γ and 40 ng of interleukin 6) and ethidium bromide (1 μg) into the dorsal white matter at T8.

2.3.3. Post-injury procedure

After injury, the muscles were sutured in layers using an absorbable 2-0 suture, and the skin was closed with a 4-0 suture. All rats were allowed to recover in a warmed cage and food and water were easily accessible. Intramuscular gentamicin (5 mg/kg) (Abbott Laboratories; Abbott Park, IL, USA) was administered immediately post-surgery and then daily for 4 days. Intramuscular buprenorphine (0.01 mg/kg using a 0.3 mg/mL preparation; Buprenex, Reckitt Benckiser Pharmaceuticals; Richmond, VA, USA) was administered post-surgery and daily thereafter for 3 days. After surgery, the rats' bladders were expressed twice per day for the first 4 days or until the rats regained control of urination. There were no complications or other infections. No sign of autotomy or autophagy were observed. The rats were maintained for 8 weeks after injury, and thereafter anesthetized and killed by transcardial perfusion with formaldehyde.

2.4. Somatosensory evoked potential recording

2.4.1. Electrode implantation

One week prior to injury, the rats were anesthetized and their head regions were shaved and aseptically prepared with chlorhexidine. Lidocaine HCl (2%) (Abbott Laboratories; North Chicago, IL,

Please cite this article in press as: Agrawal G et al. Slope analysis of somatosensory evoked potentials in spinal cord injury for detecting contusion injury and focal demyelination. *J Clin Neurosci* (2010), doi:10.1016/j.jocn.2010.02.005

USA) was injected under the skin, and an incision was made along the midline. The skull was cleaned by removing the tissue under the skin. A standard dental drill (Fine Science Tools; North Vancouver, BC, Canada) was used to drill five burr holes into the exposed part of the skull. Four holes were located on the somatosensory cortex corresponding to the hind- and forelimbs in each hemisphere. On each hemisphere, the forelimb recording sites were located 0.2 mm posterior to and 3.8 mm lateral to the bregma, and the hindlimb recording sites were located 2.5 mm posterior to and 2.8 mm lateral to the bregma. A fifth hole drilled on the right frontal bone, situated 2 mm from both the sagittal and coronal sutures, served as the intracranial reference. Transcranial screw electrodes (E363/20) (Plastics One; Roanoke, VA, USA) were then screwed into the holes such that they made very light contact with the dura mater, without causing compression of the brain tissue. The distal end of each electrode was inserted into one of the slots of an electrode pedestal (MS363; Plastics One). In order to secure the electrodes for long-term recording of cortical SEPs, carboxylate dental cement (Durelon carboxylate cement) (3 M ESPE; St. Paul, MN, USA) was used to hold the screw electrodes and the electrode pedestal in place. After the cement hardened, the skin incision was closed with a 4-0 suture.

2.4.2. Multi-limb monitoring

Subdermal needle electrode pairs (Safelead F-E3-48) (Grass Technologies; West Warwick, RI, USA) were used to electrically stimulate the median and tibial nerves of both the left and right limbs, without direct contact with the nerve bundle. An isolated constant current stimulator (DS3) (Digitimer; Welwyn Garden City, Hertfordshire, UK) was used for electrical stimulation of the limbs. A personal computer (custom-designed by Infinite Biomedical Technologies LLC, Baltimore, MD, USA) was connected to the stimulator. Custom Intraoperative Neurological Monitoring (INM) software (Infinite Biomedical Technologies LLC) was used to set the stimulation parameters and trigger the stimulator. Positive current pulses of 3.5 mA magnitude and 200 μs duration at a frequency of 1 Hz were used for limb stimulation, which sequentially stimulated each of the four limbs at a frequency of 0.25 Hz using an advanced demultiplexer circuit.

Cortical SEPs from the transcranial electrodes were amplified using an optically isolated biopotential amplifier (Opti-Amp 8002) (Intelligent Hearing Systems; Miami, FL, USA) with a gain of 30 000. The analog signal from each hemisphere was transferred to a personal computer via an optical data acquisition system with four input channels at a sampling rate of 5 kHz. Electroencephalograms (EEGs) for each hemisphere, containing the SEPs for the respective hemisphere, the stimulation pulse signal and the stimulated limb number, were recorded on separate channels for post-operative data analysis.

Contralateral SEP recordings were used for analysis. All signal processing was performed using Matlab 7.0 (MathWorks; Natick, MA, USA). The signal-to-noise ratio was improved by ensemble averaging of 100 successive stimulus-locked sweeps, with the averaging window shifting by 20 sweeps each time. The first 4 ms of an SEP signal is generally corrupted by the stimulation signal, and does not give much relevant information about spinal cord integrity, so this part of the waveform is excluded from our analysis.

2.4.3. Slope analysis of waveforms

Any waveform can be represented in a number of ways, the time domain representation being the most straightforward. However, although this representation is complete, it can be often inefficient and not directly amenable to identifying key features of interest. Hence, the waveform is often represented in a transformed domain (for example, the frequency domain) using operators that are more suitable to its analysis. We propose the use of a novel technique, involving a differential operator, for transforming the signal to allow better characterization of the entire shape of the signal. Unlike traditional SEP analysis methods, the technique bypasses the need for sophisticated peak-detection algorithms, and thus in future could bypass the need for expert intervention. This will make the proposed technique a better candidate for automation.

As mentioned in earlier sections, the normal SEP waveform (in rats as well as in humans) consists of standard peaks. SEPs by nature are low amplitude and also difficult to separate from background EEG. Furthermore, many types of neural injuries can drastically reduce the SEP in general. This can often make the peaks in SEP traces indistinct and difficult to detect due to noise or the effects of injury, hence the need for a method that can assess a given SEP independent of its peaks. The morphology of the entire signal could be a better focus for development of such a technique. The morphological information in every SEP sweep could essentially be captured if the magnitude and the slope at each instant are specified and characterized. This information can be more general than the traditional peak amplitude and location information, since the peaks can be localized by identifying the zero-crossings of the first derivative signal. Therefore, we developed a slope analysis method for the SEP waveforms.

The slope $\delta[\kappa]$ of a signal $x[\kappa]$ over two consecutive samples was computed using:

$$\delta[\kappa] = \frac{x[\kappa+1] - x[\kappa]}{(\kappa+1) - \kappa} \quad \text{for} \quad \kappa = 1, 2, \ldots, N-1, \tag{1}$$

where N is the total number of samples in a sweep. The corresponding angular orientation $\theta[\kappa]$ is then given by:

$$\theta[\kappa] = \tan^{-1}(\delta[\kappa]) \quad \text{for} \quad \kappa = 1, 2, \ldots, N-1. \tag{2}$$

The first derivative of signals is usually very noisy, as this operation amplifies high-frequency noise. To solve this problem, the slopes were binned along the waveform into time bins of L samples and the mean of the slopes $\delta_{\text{mean}}[j]$ was computed within each time bin as:

$$\delta_{\text{mean}}[j] = \frac{1}{L}\sum_{i=1}^{L} \delta[i + L \times (j-1)] \quad \text{for} \quad j = 1, 2, \ldots, M, \tag{3}$$

where $M = N/L$ is the total number of time bins in the signal. Besides decreasing noise, the binning and averaging procedure also has the advantage of reducing the dimensionality of the transformed signal, hence allowing easier computation in this lower-dimension space.

From the mean slope $\delta_{\text{mean}}[j]$, the mean angular orientation $\theta_{\text{mean}}[j]$ was obtained using Eqn (2). The array $\theta_{\text{mean}}[j]_{j=1,\ldots,M}$ is a vector in an M-dimensional space. We shall refer to this vector as the mean slope vector Θ.

To measure the similarity between any two obtained mean slope vectors Θ_i and Θ_j, the cosine distance[26] between them was computed as:

$$d(i,j) = 1 - \frac{\Theta_i{}^T \Theta_j}{\sqrt{\Theta_i{}^T \Theta_i}\sqrt{\Theta_j{}^T \Theta_j}} \tag{4}$$

The commonly used Euclidean distance is sensitive to changes in the magnitude as well as the direction of the mean slope vectors Θ_i and Θ_j. However, the shape of the signal is defined by the direction of the mean slope vector Θ alone, while its magnitude scales the waveform without affecting the overall structure of the waveform. The cosine distance better encodes this feature and hence performs better when two waveforms are compared.

A slope histogram (Supplementary Fig. 1, center panel) was constructed for the SEP signal by clustering the angular orienta-

Please cite this article in press as: Agrawal G et al. Slope analysis of somatosensory evoked potentials in spinal cord injury for detecting contusion injury and focal demyelination. *J Clin Neurosci* (2010), doi:10.1016/j.jocn.2010.02.005

tions $\theta[\kappa]_{\kappa=1,\ldots,N}$ into time bins of 2 ms and angle bins of 5°. The mean slope vectors Θ_{pre} and Θ_{post} were constructed for the SEP signals for pre-injury and post-injury stages, respectively, using L = 10, which corresponds to a duration of 2 ms, as shown in Supplementary Fig. 1 (bottom panel).

The major part of the SEP signal is concentrated between 8 ms and 28 ms, and therefore only this portion is used for all further analysis. The cosine distance between $|\Theta_{pre}|$ and $|\Theta_{post}|$ was calculated for all rats and limbs. The mean difference between the cosine distances of forelimbs (non-injured) and hindlimbs (injured) was checked for significance using Student's paired sample 2-tailed t-test.

2.4.4. Sensitivity and specificity analysis

Since the spinal cords were injured at the T8 level, the forelimb SEP signals were expected to remain constant, as the forelimb pathways were not injured. Hence, for calculating the performance measures for the analysis techniques, the forelimbs were used as the non-injured group and the hindlimbs as the injured group. Since the injury was in the midline, the right and left limb data were pooled. Therefore, 96 data points were used in total for the non-injured and injured groups (48 data points for each group).

The sensitivity of an analysis technique was calculated as the probability that the diagnostic test is positive given that the subject actually has the disease:

$$\text{sensitivity} = \frac{\text{number of true positives}}{\text{number of true positives} + \text{number of false negatives}} \quad (5)$$

The specificity was calculated as the probability that the diagnostic test is negative given that the subject does not have the disease:

$$\text{specificity} = \frac{\text{number of true negatives}}{\text{number of true negatives} + \text{number of false positives}} \quad (6)$$

The N1 latency, P2 latency and N1–P2 amplitude of the SEP signals was computed for both the pre-injury and post-injury stages. The post-injury values were then expressed as a percentage of pre-injury values to account for inter-animal variability. These percentage values were used to compute the sensitivity and specificity of the test.

The cosine distance values obtained from the slope analysis technique were also used to compute the sensitivity and specificity of the test. The best cut-off point was calculated from the receiver operating curve (ROC; sensitivity *vs* 1 – specificity) as the closest point to the (0,1) coordinate point.

3. Results

The averaged SEP signals for both pre-injury and post-injury stages in a single rat are shown in Fig. 1. The spinal cord was injured at T8, so only the hindlimb SEP signals are severely affected. There is a reduction in amplitude for both the right and left hindlimbs, accompanied by major broadening of peaks. However, no prominent effect of injury can be seen in the forelimb SEP signals.

Supplementary Fig. 2 shows examples of slope histograms and mean slope vectors for both pre-injury and post-injury stages in a single rat. In the forelimb SEP signals, the angular orientations reach high values for both stages, indicating that injury has not affected the forelimb signals. However, in the hindlimb SEP signals, the angular orientations become very small after injury as compared with those before injury. There is major broadening or disappearance of peaks in the hindlimb SEP waveforms, indicating the deleterious effect of SCI on the hindlimb signals.

Box plots for the absolute mean slope vectors $|\Theta_{pre}|$ and $|\Theta_{post}|$ for the two groups of rats, for all four limbs, are shown in Fig. 2. There are no apparent significant differences between the two stages for the forelimb SEP signals. However, for the hindlimbs, a potentially significant SEP difference between the two stages is evident.

Fig. 3 shows the cosine distances (see Eqn (4)) between pre-injury vectors $|\Theta_{pre}|$ and post-injury vectors $|\Theta_{post}|$ for all rats, for both forelimbs and hindlimbs. The mean difference between the

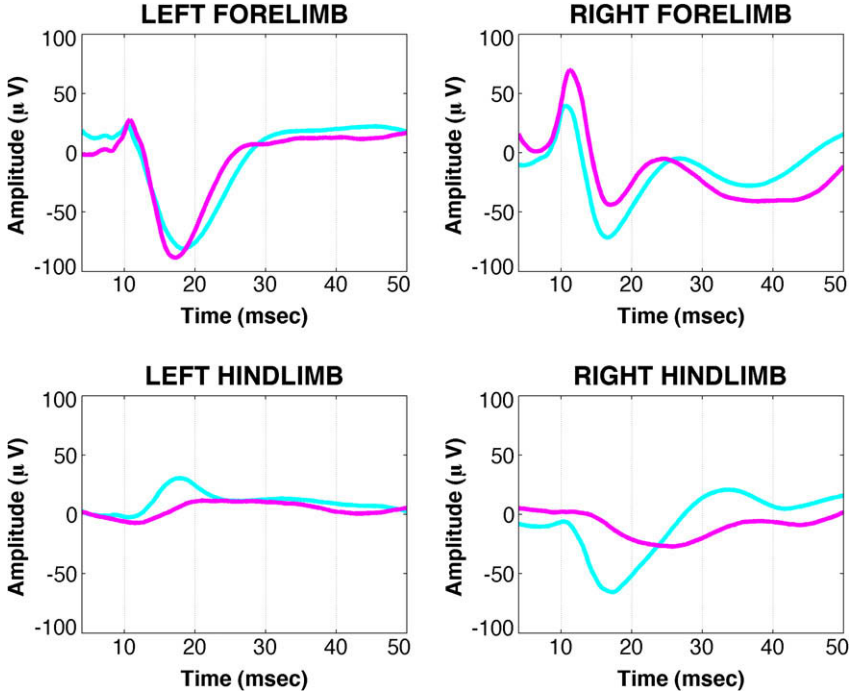

Fig. 1. Averaged somatosensory evoked potential (SEP) signals from a rat for both pre-injury (cyan/light gray) and post-injury (magenta/dark gray) stages after spinal cord injury at thoracic vertebra T8 showing that only the hindlimb SEP signals are severely affected. (This figure is available in colour at www.sciencedirect.com)

Please cite this article in press as: Agrawal G et al. Slope analysis of somatosensory evoked potentials in spinal cord injury for detecting contusion injury and focal demyelination. *J Clin Neurosci* (2010), doi:10.1016/j.jocn.2010.02.005

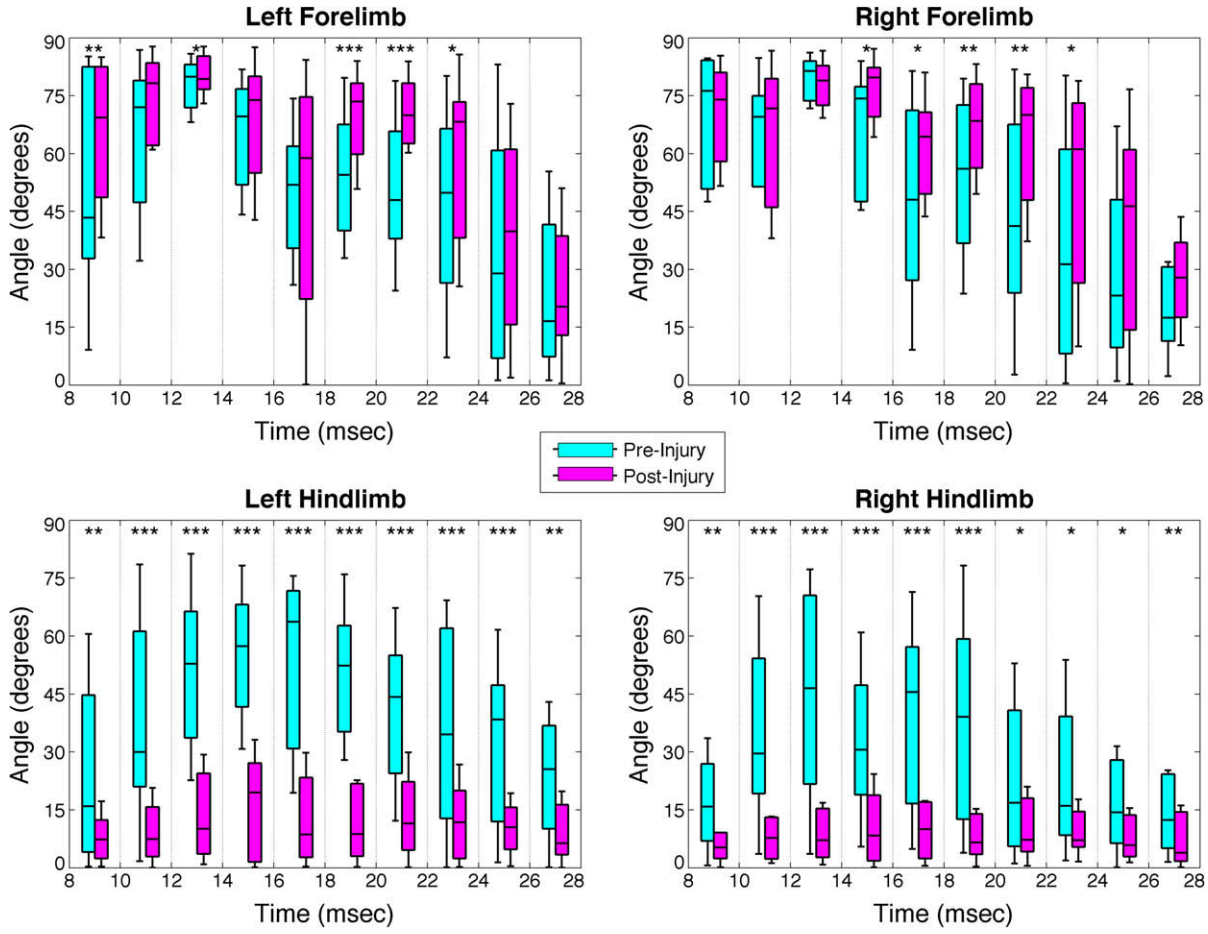

Fig. 2. Grouped box plots of absolute mean slope vectors for all rats, for both pre-injury and post-injury stages. Asterisks indicate the statistical significance of mean differences between the two stages: $^{*}p < 0.05$, $^{**}p < 0.01$, $^{***}p < 0.001$. (This figure is available in colour at www.sciencedirect.com).

cosine distances of forelimbs (non-injured) and hindlimbs (injured) was found to be strongly significant (p-value of <0.00001). An ROC curve was plotted for these cosine distance values using different cut-off points, as shown in Fig. 4. The best cut-off point was found to be 0.1491; that is, a distance of more than 0.1491 between pre-injury and post-injury signals was an indicator of injury.

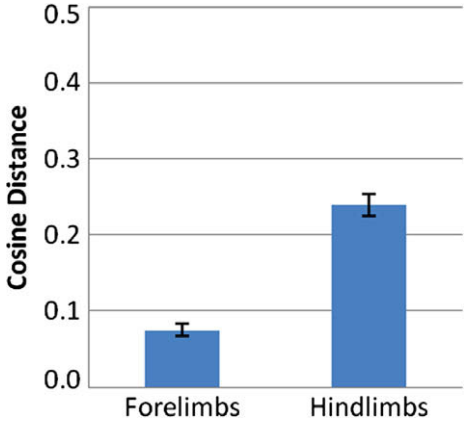

Fig. 3. Mean cosine distance of absolute mean slope vectors for both pre-injury and post-injury stages, for forelimbs and hindlimbs, for all rats. Error bars represent the standard errors for each limb.

Table 1 shows the calculation of the various performance measures of slope analysis for SCI detection using this cut-off point. It also shows the sensitivity and specificity measures of the latency and amplitude parameters. Clearly, the slope analysis technique is more sensitive and specific than the latency and amplitude parameters.

4. Discussion

Somatosensory evoked potentials can be used to reliably assess the integrity and functionality of the sensory pathways in the spinal cord. However, the peaks in these signals are not always discernible. For instance, the SEP flattens following severe SCI, resulting in especially indistinct peaks. This problem prompted us to develop a new technique that is not based on peak detection, and can be used to analyze the slope of the evoked potentials more reliably, without human intervention. The presence of peaks in a waveform is largely indicated by slopes; however, peaks are virtually instantaneous and only indicate potential inversions. They do not frame the entire signal breadth of the SEP waveform. The use of slope changes gives a more global representation of potential changes throughout the waveform.

In this paper, we propose a new slope analysis technique for SEPs, and present data demonstrating the efficacy of the technique based on SEP recordings obtained in rats before and after contusion injury or a focal EAE lesion. The method was effectively able to differentiate between the pre-injury and post-injury signals based on mean slope changes over the entire signal, with high sensitivity

Please cite this article in press as: Agrawal G et al. Slope analysis of somatosensory evoked potentials in spinal cord injury for detecting contusion injury and focal demyelination. *J Clin Neurosci* (2010), doi:10.1016/j.jocn.2010.02.005

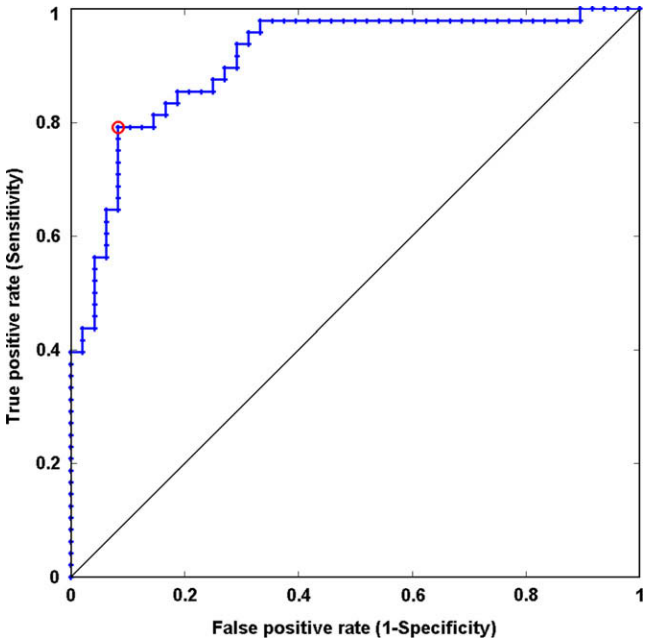

Fig. 4. Receiver operating curve using cosine distance (see Equation (4)) for spinal cord injury detection. The best cut-off point (circled) was selected on the basis of distance from the unit-slope line.

Table 1
Sensitivity and specificity of somatosensory evoked potential monitoring for spinal cord injury detection using various parameter measurements

	Sensitivity (%)	Specificity (%)
N1 latency	64.58	62.50
P2 latency	66.67	72.92
N1–P2 amplitude	68.75	45.83
Slope analysis	79.17	91.67

and specificity. Hence, using this technique it is possible to identify changes in the entire structure of the evoked potentials, as opposed to the focus on the peaks when using time-domain analysis, which does not reflect the full extent of the deformational change that occurs after injury. In conclusion, our study demonstrates the applicability, value and validity of analyzing slope changes over the entire SEP waveform, in conjunction with traditional amplitude/latency measurements of the peaks in SEP signals, to improve reliability.

Acknowledgments

This study was supported by the Maryland Stem Cell Research Fund (grants 2007-MSCRFII-0159-00 and 2009-MSCRFII-0091-00) and the Johns Hopkins Project RESTORE fund (Transverse Myelitis Research Project).

Appendix A. Supplementary material

Supplementary data associated with this article can be found, in the online version, at doi:10.1016/j.jocn.2010.02.005.

References

1. National Spinal Cord Injury Statistical Center. *Spinal cord injury: facts and figures at a glance*. <http://www.spinalcord.uab.edu/show.asp?durki=116979>; 2008 [accessed 02.10].
2. McKinley WO, Seel RT, Hardman JT. Nontraumatic spinal cord injury: incidence, epidemiology, and functional outcome. *Arch Phys Med Rehabil* 1999;**80**:619–23.
3. Bunge RP, Puckett WR, Becerra JL, et al. Observations on the pathology of human spinal cord injury: a review and classification of 22 new cases with details from a case of chronic cord compression with extensive focal demyelination. *Adv Neurol* 1993;**59**:75–89.
4. Kakulas BA. A review of the neuropathology of human spinal cord injury with emphasis on special features. *J Spinal Cord Med* 1999;**22**:119–24.
5. Fawcett J. Repair of spinal cord injuries: where are we, where are we going? *Spinal Cord* 2002;**40**:615–23.
6. Kakulas BA. Neuropathology: the foundation for new treatments in spinal cord injury. *Spinal Cord* 2004;**42**:549–63.
7. Holaday JW, Faden AI. Spinal shock and injury: experimental therapeutic approaches. *Adv Shock Res* 1983;**10**:95–8.
8. Bracken MB, Shepard MJ, Holford TR, et al. Methylprednisolone or tirilazad mesylate administration after acute spinal cord injury: 1-year follow up. Results of the third national acute spinal cord injury randomized controlled trial. *J Neurosurg* 1998;**89**:699–706.
9. Keirstead HS, Nistor G, Bernal G, et al. Human embryonic stem cell-derived oligodendrocyte progenitor cell transplants remyelinate and restore locomotion after spinal cord injury. *J Neurosci* 2005;**25**:4694–705.
10. Fehlings MG, Tator CH, Linden RD. The relationships among the severity of spinal cord injury, motor and somatosensory evoked potentials and spinal cord blood flow. *Electroencephalogr Clin Neurophysiol* 1989;**74**:241–59.
11. Brösamle C, Huber AB. Cracking the black box and putting it back together again: animal models of spinal cord injury. *Drug Discov Today. Dis Models* 2006;**3**:341–7.
12. Gruner JA. A monitored contusion model of spinal cord injury in the rat. *J Neurotrauma* 1992;**9**:123–6.
13. Noble LJ, Wrathall JR. Spinal cord contusion in the rat: morphometric analyses of alterations in the spinal cord. *Exp Neurol* 1985;**88**:135–49.
14. Onifer SM, Rabchevsky AG, Scheff SW. Rat models of traumatic spinal cord injury to assess motor recovery. *ILAR J* 2007;**48**:385–95.
15. Kerschensteiner M, Stadelmann C, Buddeberg BS, et al. Targeting experimental autoimmune encephalomyelitis lesions to a predetermined axonal tract system allows for refined behavioral testing in an animal model of multiple sclerosis. *Am J Pathol* 2004;**164**:1455–69.
16. Perot PL. The clinical use of somatosensory evoked potentials in spinal cord injury. *Clin Neurosurg* 1973;**20**:367–81.
17. Perot PL, Vera CL. Scalp-recorded somatosensory evoked potentials to stimulation of nerves in the lower extremities and evaluation of patients with spinal cord trauma. *Ann N Y Acad Sci* 1980;**338**:359–68.
18. Sedgwick EM, el-Negamy E, Frankel H. Spinal cord potentials in traumatic paraplegia and quadriplegia. *J Neurol Neurosurg Psychiatry* 1980;**43**:823–30.
19. Rowed DW, McLean JA, Tator CH. Somatosensory evoked potentials in acute spinal cord injury: prognostic value. *Surg Neurol* 1978;**9**:203–10.
20. Cracco RQ. Spinal evoked response: peripheral nerve stimulation in man. *Electroencephalogr Clin Neurophysiol* 1973;**35**:379–86.
21. Dorfman LJ, Perkash I, Bosley TM, et al. Use of cerebral evoked potentials to evaluate spinal somatosensory function in patients with traumatic and surgical myelopathies. *J Neurosurg* 1980;**52**:654–60.
22. American Electroencephalographic Society. Guideline eleven: guidelines for intraoperative monitoring of sensory evoked potentials. *J Clin Neurophysiol* 1994;**11**:77–87.
23. Nuwer MR, Daube J, Fischer C, et al. Neuromonitoring during surgery: report of an IFCN committee. *Electroencephalogr Clin Neurophysiol* 1993;**87**:263–76.
24. Agrawal G, Sherman D, Thakor N, et al. A novel shape analysis technique for somatosensory evoked potentials. In: *Conference Proceedings of the Annual Meeting of the IEEE Engineering in Medicine and Biology Society*. Piscataway, NJ, USA; IEEE, 2008. p. 4688–91.
25. Mahmoudi F, Shanbehzadeh J, Eftekhari-Moghadam AM, et al. Image retrieval based on shape similarity by edge orientation autocorrelogram. *Pattern Recog* 2003;**36**:1725–36.
26. Lee L. Measures of distributional similarity. In: *Proceedings of the 37th Annual Meeting of the Association for Computational Linguistics*, College Park, Maryland. Association for Computational Linguistics, IL, USA; Stroudsburg, 1999. p. 25–32.